Block Decimation Renormalization Group and Finite Range Scaling Method to Analyze Infinitely Long Range Interacting 1-Dimensional Systems*)

Ken-Ichi Aoki**), Tamao Kobayashi***) and Hiroshi Tomita†)

Institute for Theoretical Physics, Kanazawa University
Kanazawa 9201192, JAPAN

To study dissipative quantum mechanics we adopt the Caldeira-Leggett model where environmental harmonic oscillators are coupled to the target variable. After integrating out the environmental degrees of freedom, effective interactions of infinitely long range appear. As the simplest example we take 2-state model for the target variable, and then we investigate the 1-dimensional Ising model with long range interactions.

We propose a new practical method to evaluate the critical coupling constant of the system for the spontaneous magnetization. First, we exactly calculate the system with finite range interactions by formulating the block decimation renormalization group method. Then, we assume a finite range scaling and define its exponent for the logarithm of susceptibility. Using this exponent, we can find the criticality with a high precision through the zeta function singularity. We obtain the phase diagram on the 2-dimensional plane spanned by the damping rate exponent and the total coupling constant of the power damping long range interactions.

§1. Introduction

The aim of this article is to propose a new practical method to evaluate the criticality of the system where the infinite range interactions are essential.

The system we consider here is the 1-dimensional Ising model. It has no phase transition at finite coupling constants (at finite temperature) if the interactions are finite range, that is, the maximum distance of spins which are directly coupled in the Hamiltonian is finite. However, if the interaction range becomes infinite, it can have the ferromagnetic phase transition.

Here we take a simple form of power damping long range interactions,

$$\beta H = -\sum_{n=1}^{\infty} \frac{\eta}{n^p}\ \sigma_i \sigma_{i+n}\ , \tag{1·1}$$

where η controls the total strength and p controls the damping rate. The existence condition of the phase transition for p has been known as,[9)]

$$1.0 < p \leq 2.0\ , \tag{1·2}$$

*) Talk given at the Workshop on Applications of Renormalization Group Methods in Mathematical Sciences, Sep.12–14, 2007, Research Institute for Mathematical Science, Kyoto. This talk was presented by Tamao Kobayashi.

**) aoki@hep.s.kanazawa-u.ac.jp

***) ballblue@hep.s.kanazawa-u.ac.jp

†) t_hirosi@hep.s.kanazawa-u.ac.jp

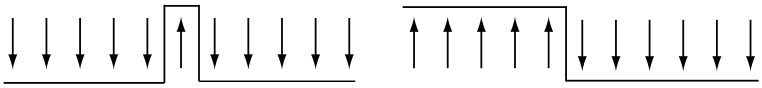

(a) (b)

Fig. 1. Understanding the conditions for p.

that is, for p in the above interval, there exists a finite critical coupling constant $\eta_{\rm c}$.

This condition for p is simply understandable as follows. For $p \leq 1.0$, consider a state of completely ordered spins and flip only one spin (Fig.1(a)). Then such state has an infinite energy and no way to realize any spin flip. Thus the system is completely ordered.

For $p > 2.0$, consider a state where the left half spins are up and the right half spins are down (Fig.1(b)). This state with one domain wall has a finite energy. Thus there is no way of developing spin expectation value, and the system is completely disordered. In between these two boundaries, there may be a finite criticality for the coupling constant η, which has been proved rigorously.[9)]

Our purpose here is to numerically calculate the value of $\eta_{\rm c}$ as a function of p. The boundary case of $p = 2$ is called Ohmic case and it has some subtleties which will be seen also by our analysis.

Before going ahead, we recapitulate the physical motivation to consider such systems. Our physical target is the dissipative quantum mechanics, which has drawn much attention for a long time. Recently experiments observing the quantum decoherence have enhanced the interest for such systems. We need deeper theoretical understanding to describe decoherence phenomena in various environments.

Dissipative systems are not easy to handle in quantum mechanics. Let us remember that classical mechanics may deal with dissipative effects, for example, by just adding a velocity dependent resisting force to the equation of motion,

$$\frac{d^2q(t)}{dt^2} = -\frac{\partial V(q(t))}{\partial q} - \eta\frac{dq(t)}{dt} \ , \tag{1·3}$$

where η is the friction coefficient. This method is actually dealt in high school physics and this type of equation of motion are applied to many realistic cases successfully. However it has been known that there is no simple and general Lagrange function for such velocity dependent resisting force.

On the other hand quantum mechanics needs Lagrangian or Hamiltonian to completely define the dynamics and to solve the system effectively. Equation of motion of operators only are not enough to handle the system. However, just as in the case of classical mechanics, it is quite non-trivial to set up an appropriate simple Hamiltonian, if we work only with the target degrees of freedom.

Instead, we should get back to the microscopic origin of dissipative phenomena.[2)] Starting with a dynamical system in which a target variable is surrounded by many environmental degrees of freedom. Then the energy flow from the target system to the environment might show up as energy dissipation effects. Modeling this concept, we prepare infinitely many harmonic oscillators which are linearly coupled to the

target system, and we integrate out these environmental degrees of freedom. Then we obtain effective interactions for the target system variable, which are in general infinitely long range and may effectively work as dissipation.

Decoherence phenomena has been argued with the double-well potential by observing the Rabi oscillation which is driven by the quantum tunneling. Due to the dissipative effects, decoherence appears to suppress the oscillation. This is seen as tunneling suppression, or localization phase transition, due to long range interactions.

The quantum double-well system with long range interactions have been studied by many authors. Typically, canonical method,[3] non-perturbative renormalization group,[5] and sophisticated Monte Carlo simulation.[6] It is very hard to fully analyze the system and is frequently approximated by the smallest degrees of freedom, that is, two state approximation. Then the system is nothing but the 1-dimensional Ising model with long range interactions.

The long range Ising model has its own long history of research. Here, we only refer to old initiating works[7,8] and a recent paper.[9] If the interaction range is finite, then the system has no phase transition and there is no ordered state. However, when the interaction range is infinite and strong enough, there can be a phase transition to give rise to the spontaneous magnetization. Actually it is not easy to evaluate the value of the critical coupling constant and it needs large size simulation even for the Ising case to get conclusive results.[10]

In the following sections we present a new practical method to evaluate the critical coupling constant in case of infinitely long range interactions. The method consists of two parts. First we limit the range of interactions to be a finite n, and solve the system precisely by using an extended type of the decimation renormalization group which we call Block Decimation Renormalization Group (BDRG).

Then we assume a scaling relation, the Finite Range Scaling (FRS). We define an exponent for the range n dependence of physical quantities and evaluate the exponent. Using the obtained FRS exponent we estimate infinite range property of the system, where the zeta function appears and its singularity structure determines the criticality. This FRS method can be seen as an alike of the finite size scaling method used in the simulation on finite lattice systems in order to guess the infinite size physics.

The FRS method can be applied to any infinite range interaction system when finite range interactions are to be effectively and precisely evaluated. Application of this method to the double-well dissipative quantum mechanics will be reported elsewhere.[11]

§2. The Caldeira-Leggett Model

Caldeira and Leggett formulated dissipative effects from a microscopic action. The model consists of a target system and the environment of infinitely many degrees

of freedom. The microscopic action of the model is written as follows,

$$S[q,\{x_\alpha\}] = \int dt\ \left\{ \frac{1}{2}M\dot{q}^2 - V_0(q) + \sum_\alpha \left[\frac{1}{2}m_\alpha \dot{x}_\alpha^2 - \frac{1}{2}m_\alpha\omega_\alpha^2 x_\alpha^2 - qC_\alpha x_\alpha \right] \right\} , \quad (2\cdot1)$$

where $q(t)$ is the variable of the target system in a potential $V_0(q)$, $x_\alpha(t)$ are the infinite number of harmonic oscillators. The target variable is coupled linearly to each oscillator with coupling constant C_α.

Environmental degrees of freedom x_α can be path integrated out, and effective interactions of target system is obtained. The effective interactions are non-local in the direction of time. Taking the Euclidean time formulation, the quantum mechanics is regarded as 1-dimensional statistical system. Then this is a 1-dimensional statistical system with infinitely long distance interaction, whose strength and dependence on distance are determined by the state density function of environmental degrees of freedom which is mentioned later. By these long range interactions, quantum mechanical nature is suppressed, and the classical behavior emerges. In terms of statistical mechanics, it corresponds to the existence of critical dissipation which develops the spontaneous breakdown of original symmetry, for example, the Z_2 parity in case of a double-well potential system.

Before proceeding to the path integral treatment, we solve the model in the classical mechanics, and show that a dissipation effect may effectively appear in the dynamics of $q(t)$. Equations of motion of $q(t), x_\alpha(t)$ given by (2·1) are written as

$$M\ddot{q} = -\frac{\partial V_0}{\partial q} - \sum_\alpha C_\alpha x_\alpha , \quad (2\cdot2)$$

$$m_\alpha \ddot{x_\alpha} = -m_\alpha\omega_\alpha^2 x_\alpha - qC_\alpha . \quad (2\cdot3)$$

We solve the second equation (2·3) first where $q(t)$ is regarded as an external force. Using the standard technique, the general solution of $x_\alpha(t)$ is obtained as

$$x_\alpha(t) = C_+ e^{i\omega_\alpha t} + C_- e^{-i\omega_\alpha t} + \int_{-\infty}^{\infty} \frac{d\omega}{2\pi} e^{-i\omega t} \frac{C_\alpha \tilde{q}(\omega)}{m_\alpha\left[(\omega+i\epsilon)^2 - \omega_\alpha^2\right]} . \quad (2\cdot4)$$

The first two terms including complex constants C_+, C_- represent a general solution of the homogeneous equation and the third term is a special solution using the retarded Green function where $\tilde{q}(\omega)$ is the Fourier component of $q(t)$ defined by

$$q(t) = \int_{-\infty}^{\infty} \frac{d\omega}{2\pi} e^{-i\omega t}\tilde{q}(\omega) . \quad (2\cdot5)$$

Now we set the initial boundary condition for $x_\alpha(t)$ by

$$x_\alpha(t=-\infty) = 0 . \quad (2\cdot6)$$

Because we also assume that the target variable should vanish at the infinite past, the special solution part vanishes, and the coefficients of a general homogeneous solution are determined as

$$C_+ = 0 , \quad C_- = 0 . \quad (2\cdot7)$$

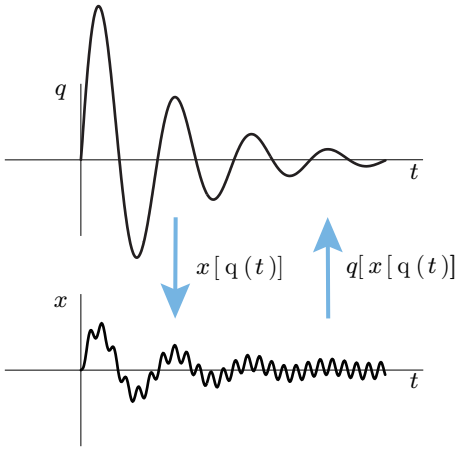

Fig. 2. Environmental back reaction works as dissipation.

Therefore $x_\alpha(x)$ has no component of the homogeneous solution.

Next we substitute the solution $x_\alpha(x)$ into the equation of motion of $q(t)$ (2·3),

$$M\ddot{q} = -\frac{\partial V_0}{\partial q} - \int_{-\infty}^{\infty} \frac{d\omega}{2\pi} e^{-i\omega t} \tilde{q}(\omega) \sum_\alpha \frac{C_\alpha^2}{m_\alpha} \frac{1}{(\omega + i\epsilon)^2 - \omega_\alpha^2} \ . \tag{2·8}$$

The second term gives a non-trivial feed back effects to the target motion.

Here we introduce the spectral density function $J(\omega)$ which characterizes the environmental degrees of freedom,

$$J(\omega) = \sum_\alpha \frac{C_\alpha^2}{4m_\alpha\omega_\alpha} (2\pi)\delta(\omega - \omega_\alpha) \ . \tag{2·9}$$

Using this function, the equation of motion of $q(t)$ (2·8) is rewritten as fellows,

$$M\ddot{q} = -\frac{\partial V_0}{\partial q} - \int_{-\infty}^{\infty} \frac{d\omega}{2\pi} e^{-i\omega t} \tilde{q}(\omega) \int_0^{\infty} \frac{d\omega'}{2\pi} J(\omega') \frac{4\omega'}{(\omega + i\epsilon)^2 - \omega'^2} \ . \tag{2·10}$$

For example, we take a linear spectral function $J(\omega) = \eta\omega$, and the back reaction part of equation (2·10) becomes,

$$\int_0^{\infty} \frac{d\omega'}{2\pi} J(\omega') \frac{4\omega'}{(\omega + i\epsilon)^2 - \omega'^2} = -4\eta \int_0^{\infty} \frac{d\omega'}{2\pi} \left[1 + \frac{\omega^2}{\omega'^2 - (\omega + i\epsilon)^2} \right] \ . \tag{2·11}$$

We apply an ultraviolet cutoff ω_c of the environmental oscillator frequencies to the first divergent integral, and integrate the second term exactly. Finally the effective equation of motion takes the following form,

$$M\ddot{q} = -\frac{\partial}{\partial q}(V_0 - \frac{\eta\omega_c}{\pi} q^2) - \eta\dot{q} \ . \tag{2·12}$$

The divergent term gives a correction to the original potential which should be called the "mass renormalization", and the additional term appears as the Ohmic

type dissipation, a resisting force proportional to the velocity. This is why the linear $J(\omega)$ function case is called Ohmic.

Note that the dissipative effects breaking the time reversal symmetry of the original Lagrangian finally emerges, and its origin is the special boundary condition we set in Eq.(2·6). The effect comes from the back reaction of the environmental degrees of freedom (see Fig.2). To make the effects dissipative, we need infinite number of degrees of freedom, since if it is finite, the system must come back to the original configuration as nearly as desired in a finite period, that is, the energy is returned to the target variable.

Next, we analyze the system quantum mechanically. We can proceed with the Heisenberg operator equation of motion which is parallel to the classical mechanics. However, in such method, we do not know a good approximation to solve the system with a non-trivial potential of the target variable. Here we take another way of formulating quantum mechanics which is appropriate for non-perturbative approximation, the (Euclidean) path integral formalism.

From the Caldeira-Leggett microscopic action (2·1), we first path integrate out all environmental variables and obtain an effective action for the target variable,

$$\Delta S[q] = -\int d\tau \int ds q(\tau)\alpha(\tau - s)q(s) \ , \tag{2·13}$$

where τ, s are Euclidean time arguments, and the coupling function is given by

$$\alpha(\tau - s) \equiv \int \frac{dE}{2\pi} \sum_\alpha \frac{C_\alpha^2}{2m_\alpha} \frac{1}{E^2 + \omega_\alpha^2} e^{iE(\tau - s)} = \sum_\alpha \frac{C_\alpha^2}{2m_\alpha} \frac{1}{2\omega_\alpha} e^{-\omega_\alpha |\tau - s|} \ . \tag{2·14}$$

Its Fourier transform takes the following form

$$\tilde{\alpha}(E) = \sum_\alpha \frac{C_\alpha^2}{2m_\alpha} \frac{1}{E^2 + \omega_\alpha^2} \ . \tag{2·15}$$

This representation is familiar for particle physicists since this is nothing but the Feynman rule making the effective interactions, the propagator of harmonic environmental variables with coupling constants at both ends where external legs of the target variable are attached.

The effective action ΔS can be decomposed into the local component in time ΔS_L and the genuine non-local component ΔS_{NL},

$$\Delta S[q] = \Delta S_L + \Delta S_{NL} \ , \tag{2·16}$$

$$\Delta S_L[q] = -\tilde{\alpha}(E = 0) \int d\tau q^2(\tau) \ , \tag{2·17}$$

$$\Delta S_{NL}[q] = \frac{1}{2} \int d\tau \int ds (q(\tau) - q(s))^2 \alpha(\tau - s) \ , \tag{2·18}$$

where we have used the following trick,

$$q(\tau)q(s) = \frac{1}{2}(q^2(\tau) + q^2(s)) - \frac{1}{2}(q(\tau) - q(s))^2 \ . \tag{2·19}$$

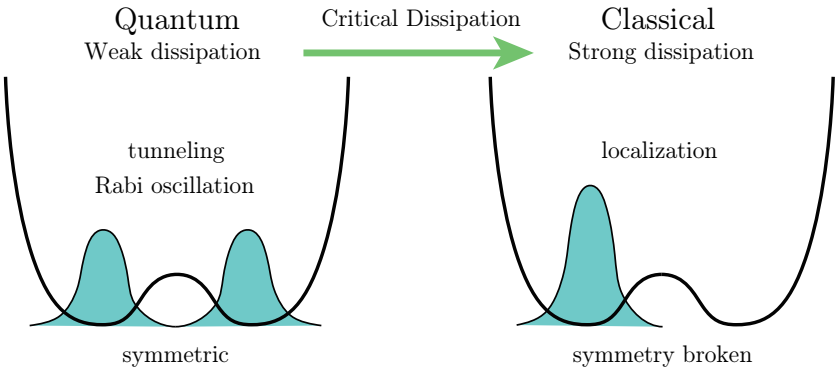

Fig. 3. Quantum-classical transition due to dissipation.

If we set ohmic dissipation $J(\omega) = \eta\omega$, these effective interactions take the following expressions,

$$\Delta S_L[q] = \int d\tau \left[-\frac{\eta}{\pi}\omega_c\right] q^2(\tau) \ , \tag{2·20}$$

$$\Delta S_{NL}[q] = \frac{1}{2}\int d\tau \int ds \frac{(q(\tau)-q(s))^2}{|\tau - s|^2} \ , \tag{2·21}$$

where ω_c is the ultraviolet cutoff of ω defined before. The non-local term ΔS_{NL} corresponds to the dissipation term in the classical treatment. Now it is long range interactions inversely proportional to the square of distance. Hereafter we consider cases with a general inverse damping power p, and we define the non-local effective action as

$$\Delta S_{\rm NL}[q] = \frac{\eta}{4\pi}\int d\tau \int ds \ \frac{(q(\tau)-q(s))^2}{|\tau - s|^p} \ . \tag{2·22}$$

Thus we analyze such long range interactions parameterized by the coupling constant η and the inverse damping power p.

Quantum dissipation has been usually analyzed in the case that the target variable potential $V_0(q)$ is a double well potential. If the coupling constant η is small it does not affect the basic quantum nature that the vacuum state is symmetric due to the tunneling and the Rabi oscillation occurs for a localized initial state, as seen in Fig.3 left. However when the dissipative interactions become strong enough, it is expected that the tunneling is suppressed and the classical nature appears through the localizing state as Fig.3 right. This transition controlled by the coupling constant η may be called as *Quantum-Classical phase transition* and there is a critical dissipation $\eta_{\rm c}$.

In the Euclidian path integral formalism, the system is treated as a 1-dimensional statistical system. There is absolutely no spontaneous symmetry breakdown, assuming that the interactions are not long range. Long range interactions break the base of the general no-go theorem and it is expected that enough strong long range interactions can develop spontaneous symmetry breakdown.

To analyze the double well quantum mechanics is difficult, we approximate the model by a simplest one, that is, just two states at each site, the Ising model, whose

statistical weight is given by

$$\beta H = \frac{\eta}{2} \sum_{i<j} \frac{(\sigma_i - \sigma_j)^2}{(i-j)^p} \ . \tag{2·23}$$

The Ising variable σ takes 1 or -1. These interactions are equivalent to the following form which will be used in this article,

$$\beta H = -\eta \sum_{i<j} \frac{\sigma_i \sigma_j}{(i-j)^p} = -\sum_i \sum_{j=1}^{\infty} K_j \sigma_i \sigma_{i+j} \ , \quad K_j = \frac{\eta}{n^p} \ . \tag{2·24}$$

For these 1-dimensional Ising model with power damping long range interactions, there have been various rigorous arguments and results especially for the existence of the finite critical coupling constant and behaviors of magnetization and susceptibility (see an excellent paper[9] and references therein).

§3. Block Decimation Renormalization Group

We will work with the 1-dimensional Ising model whose action is defined by

$$S = -\sum_i \sum_{j=1}^{\infty} K_j \sigma_i \sigma_{i+j} - h \sum_i \sigma_i \ , \tag{3·1}$$

where each spin variable σ_i takes 1 or -1, and h is an external field to calculate magnetization susceptibility. The coupling constants K_j, assumed to be non-negative, determine the interactions between spins of distance j.

As a first step we take the nearest neighbor model where only K_1 is non-vanishing. Interactions are represented by 2×2 matrix (sometimes called the transfer matrix) of the following form,

$$T^{(0)} = \begin{pmatrix} \exp(K_1 + h) & \exp(-K_1) \\ \exp(-K_1) & \exp(K_1 - h) \end{pmatrix} \ . \tag{3·2}$$

We define the Decimation Renormalization Group (DRG) transformation by integrating out all the even site spins and define effective interactions among odd site spins.[1),4)] The effective interactions still takes the nearest neighbor form. Thus this renormalization procedure can be iterated and we define k-th renormalized interactions $T^{(k)}$ by induction,

$$T^{(k)} \equiv T^{(k-1)} \ T^{(k-1)} \ , \tag{3·3}$$

which are interactions for spins on sites of spacing 2^k.

We can calculate the partition function for the finite size system with periodic boundary condition (corresponding to a finite temperature case for the original quantum mechanical model) by

$$Z^{(k)} = \mathrm{Tr} \ T^{(k)} \ . \tag{3·4}$$

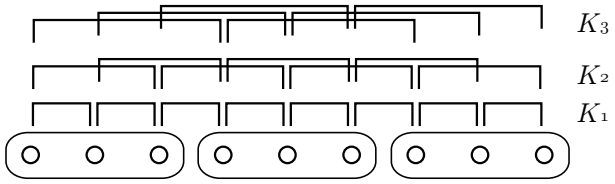

Fig. 4. Example of spin blocks. Take $n = 3$ as maximum range and organize blocks made of 3-spins each. Inter-block interactions are limited to those between nearest neighbor blocks.

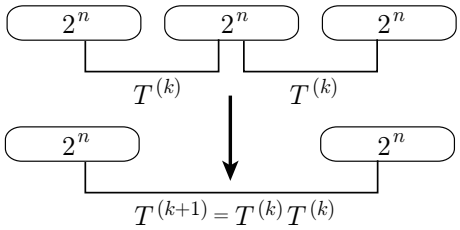

Fig. 5. Block decimation renormalization group transformation.

The system size here is 2^k and we have the free energy per site,

$$F^{(k)} = \frac{1}{2^k} \log \mathrm{Tr}\ T^{(k)} \ . \tag{3·5}$$

Differentiating the above free energy density with respect to the external field h, we have the susceptibility χ of the finite system,

$$\chi^{(k)} = \frac{1}{2^k} \frac{\partial^2}{\partial h^2} \log \mathrm{Tr}\ T^{(k)} \Big|_{h=0} \ . \tag{3·6}$$

Finally the large k limit gives us the susceptibility of the infinite size (zero temperature in the original quantum mechanics) system. In this simplest case, the zero temperature susceptibility is exactly calculated as,

$$\chi^{(\infty)} = \lim_{k\to\infty} \frac{1}{2^k} \frac{\partial^2}{\partial h^2} \log \mathrm{Tr}\ T^{(k)} \Big|_{h=0} = \exp(2K_1) \ . \tag{3·7}$$

Then we proceed to include non-nearest neighbor interactions, but we still limit the interaction range to be n, that is, $K_j = 0$ for $j > n$. This is the first stage of our new method, the Finite Range Scaling (FRS). The standard DRG does not work well any more. To solve this system we divide spins into blocks of size n as shown in Fig.4. Then the interactions are all limited to "nearest neighbor" inter-block interactions. Thus the system is a one dimensional nearest neighbor block-spin system.

One block contains n spins and it accommodates totally 2^n states. The inter-block interactions are represented by $2^n \times 2^n$ matrix. The renormalization group transformation is defined for this block-spin matrix (see Fig.5), which we call Block Decimation Renormalization Group (BDRG).[11] Numerical calculation of BDRG gives us a precise value of the susceptibility of the system with range n interactions, which we denote $\chi(n)$.

§4. Approximation of Block Decimation Renormalization Group

We investigate approximation of BDRG to take a subspace of the total interaction space. This is a standard systematic approximation scheme in the analysis of non-perturbative renormalization group.[4] Its validity is evaluated by comparing it with numerical calculations by BDRG.

In the case that nearest neighbor interaction is strong enough, the correlation between neighboring spins should be very high. Taking account of this situation, we keep only 2 states, among 2^n states, in which all spins in a block take the same direction,

$$\Uparrow \equiv \uparrow\uparrow \cdots \uparrow\uparrow \ , \quad \Downarrow \equiv \downarrow\downarrow \cdots \downarrow\downarrow \ , \tag{4·1}$$

and we expect this approximation would be good for strong coupling region. Then the dimension of reduced T matrix is 2×2. This approximation here is defined by reducing the independent states of each block and it seems different from the usual way of projecting the renormalization group flow onto a subspace of interactions. However the elements of T matrix represents a point in the total interaction space of dimension 2^{2n} except for reduction due to its mirror image symmetry, and if we set all other elements than those including the above two states to be vanishing, then such subspace becomes an invariant subspace of the renormalization group flow. Any subset of block states defines a subspace of renormalization group flow. From this viewpoint, this approximation here can be regarded as one of the standard approximation methods of the non-perturbative renormalization group.

We name this approximation as Aligned BDRG (ABDRG). We take notice of microscopic (bare) T matrix. Because the effects of interactions within a block are same for all 4 configurations, those in-block effects are factored out without changing the structure of the 2×2 matrix form. Then it turned out that the bare T matrix in ABDRG depends only on the following effective coupling constant defined by a special linear combination of all coupling constants,

$$K_{\text{eff}}^{[\text{S}]} \equiv \sum_{m=1}^{n} m K_m \ , \tag{4·2}$$

where the suffix [S] in $K_{\text{eff}}^{[\text{S}]}$ indicates the strong interaction regime. Using this effective coupling constant, the bare T matrix is given by the following two elements,

$$T_{\Uparrow\Uparrow}^{(0)} = T_{\Downarrow\Downarrow}^{(0)} = \exp(K_{\text{eff}}^{[\text{S}]}) \ , \quad T_{\Uparrow\Downarrow}^{(0)} = T_{\Downarrow\Uparrow}^{(0)} = \exp(-K_{\text{eff}}^{[\text{S}]}) \ . \tag{4·3}$$

Adding the external field h we have the bare T matrix in ABDRG as follows,

$$T^{(0)} = \begin{pmatrix} \exp(K_{\text{eff}}^{[\text{S}]} + nh) & \exp(-K_{\text{eff}}^{[\text{S}]}) \\ \exp(-K_{\text{eff}}^{[\text{S}]}) & \exp(K_{\text{eff}}^{[\text{S}]} - nh) \end{pmatrix} \ . \tag{4·4}$$

This form is quite similar to the nearest neighbor model, so the solutions of the renormalization group equation is given analytically.

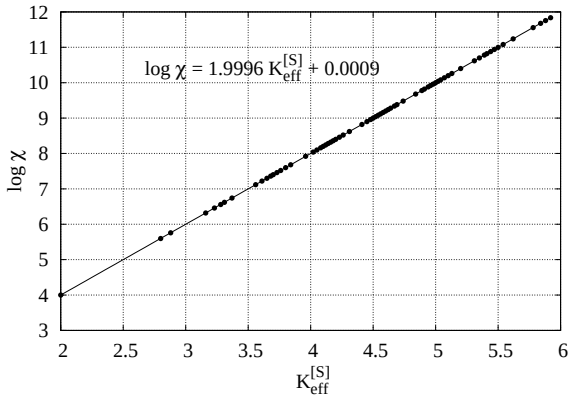

Fig. 6. BDRG exact calculation of the logarithm of the susceptibility.

To evaluate the susceptibility, we first calculate the magnetization under external field,

$$M^{(k)}(h) = \frac{T_{11}^{(k)} - T_{22}^{(k)}}{T_{11}^{(k)} + T_{22}^{(k)}} \ . \tag{4·5}$$

We differentiate it with respect to the external field so as to obtain the susceptibility. After taking the zero temperature limit, we have

$$\chi^{(\infty)} = \left. \frac{\partial M^{(\infty)}(h)}{\partial h} \right|_{h=0} = n \exp(2K_{\rm eff}^{[\rm S]}) \ . \tag{4·6}$$

As a result, the logarithm of the susceptibility is linear in $K_{\rm eff}^{[\rm S]}$,

$$\log(\chi^{(\infty)}) = 2K_{\rm eff}^{[\rm S]} + \log(n) \ . \tag{4·7}$$

The important feature is that only one effective coupling constant defined by a special linear combination of original coupling constants controls the system completely.

We compare the above result with the numerical analysis of BDRG. We set the maximum interaction distance to be 6, and take many cases of random coupling constants for each distance. We numerically solve the exact BDRG, and estimate the logarithm of the susceptibility. The dependence on the effective coupling constant is plotted in Fig.6. Because it is necessary that the nearest neighbor interaction is strong for ABDRG, the nearest neighbor coupling constant is limited to be larger than 2. We see the exact linear dependence only on the effective coupling constant. Thus the prediction by ABDRG is exact for this linear term. However the constant term, $\log n$ in Eq.(4·7), seems incorrect, and it should be fixed since we are finally interested in the limit $n \to \infty$.

In ABDRG, we do not allow spin flip in a block while spin may flip at the boundary between blocks. We guess that the overestimate of susceptibility in ABDRG comes from the shortage of the instanton entropy because of the above limitation.

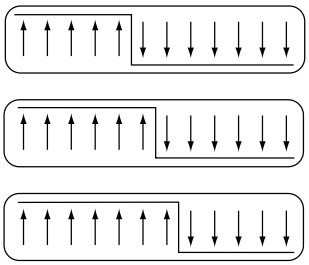

Fig. 7. N-ABDRG allows spin flip once in a block.

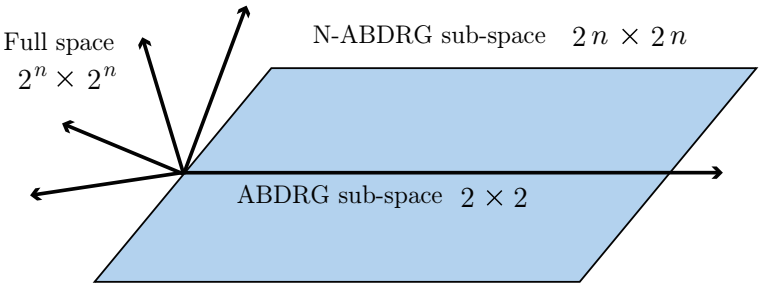

Fig. 8. Interaction space of BDRG and its approximation subspace.

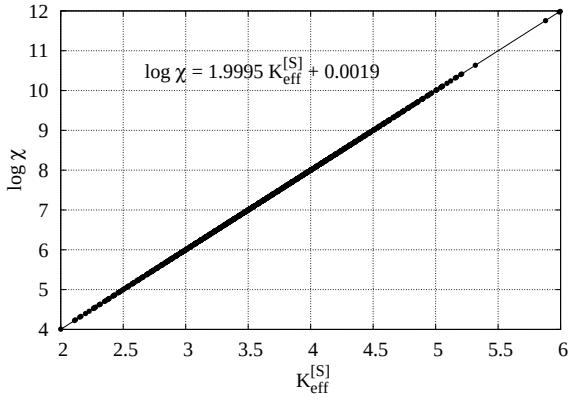

Fig. 9. N-ABDRG results of the logarithm of the susceptibility.

We try enlargement of the renormalization group flow subspace in order to compensate this shortage. We add spin flip degrees of freedom within a block. Actually, we allow spin flip just once within a block as Fig.7. Then the number of states in a block increases to be $2n$. We call this approximation as Next-to-ABDRG (N-ABDRG).

This enlargement of subspace for the renormalization group flows also belongs to the usual scheme of improving approximations in non-perturbative renormalization group method.[4] As drawn in Fig.8, BDRG interaction space has $2^n \times 2^n$ dimension, which is the full theory space. In ABDRG, we restrict the space to be 2×2 dimension A-subspace, which is drawn by a line. In N-ABDRG, we improve the interaction space and increase its dimension to be $2n \times 2n$, the NA-subspace drawn by a plane.

Numerical results of N-ABDRG is shown in Fig.9. We calculated over 2000 cases of random coupling constants. As for the linear dependence of logarithm of the susceptibility of the effective coupling constant, N-ABDRG is perfectly correct including the constant term, that is, $\log n$ term in ABDRG vanishes.

§5. Inequalities for the Logarithm of Susceptibility

Here we propose two inequalities for the logarithm of susceptibility,

$$2K_{\rm eff}^{[\rm W]} \leq \log \chi \leq 2K_{\rm eff}^{[\rm S]} \ . \tag{5·1}$$

Two effective coupling constants, good for weak and strong regions respectively, are defined by

$$K_{\rm eff}^{[\rm W]} \equiv \sum_j K_j \ , \quad K_{\rm eff}^{[\rm S]} \equiv \sum_j j K_j \ . \tag{5·2}$$

They have been called 0th and 1st moments of coupling constants in references and have played crucial roles to determine phase structures. We propose these inequalities should hold for any set of non-negative coupling constants K_j. Though we have not yet succeeded in rigorously proving these inequalities, we did find no exception against them in our calculation by BDRG.

We show numerical confirmation for these inequalities in Fig.10 and Fig.11. Figure.10 is a lower bound check for random coupling constants and Fig.11 is an upper bound check. As far as we see the results, these inequalities are valid for any set of coupling constants.

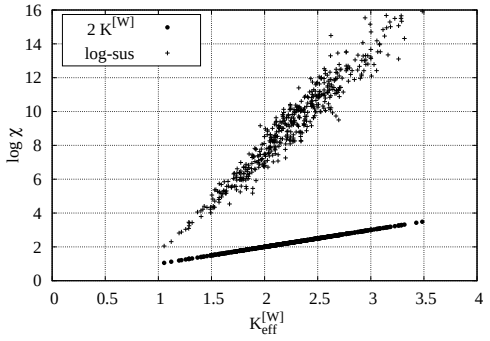

Fig. 10. Random coupling constant check of the susceptibility lower bound.

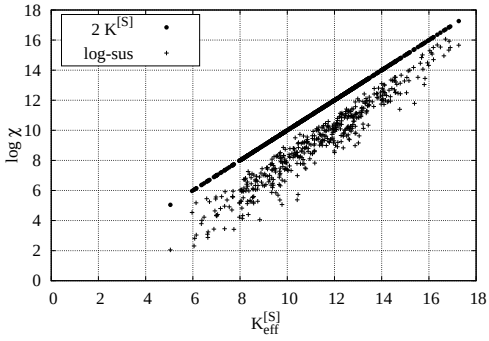

Fig. 11. Random coupling constant check of the susceptibility upper bound.

Physical pictures for these two bounds are the followings. The weak bound $2K_{\rm eff}^{[\rm W]}$ comes from the 1st order perturbation expansion of the logarithm of the susceptibility. Probably some convexity in the weak region assures the bound. The strong bound comes from the case of almost ordered situation, where an approximate of BDRG equation, NABDRG, describes the system well and it gives the boundary value $2K_{\rm eff}^{[\rm S]}$. In case of the nearest neighbor model, both equalities hold exactly and simultaneously.

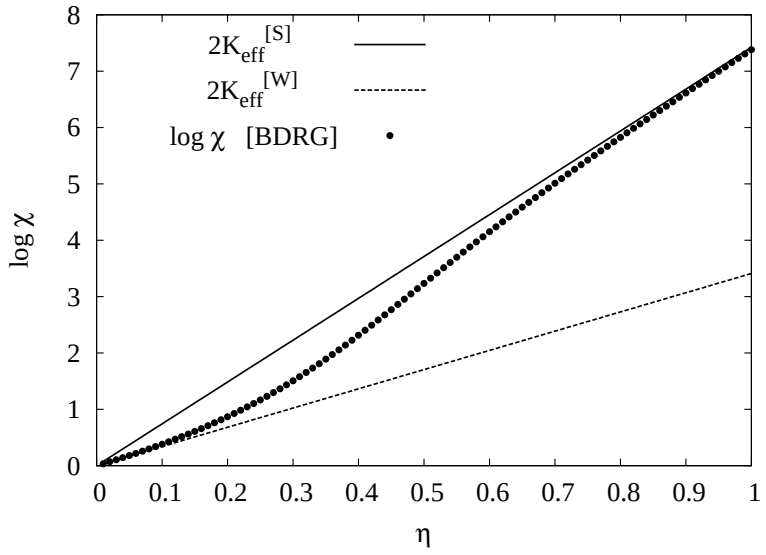

Fig. 12. Susceptibility for $p = 1.8, \eta = [0, 1]$ and $n = 11$, with predicted boundaries

Now we get back to the case with the power damping series of coupling constants K_j parameterized as

$$K_j = \frac{\eta}{j^p} \ . \tag{5·3}$$

For this power damping series of coupling constants, the inequalities read

$$2\eta\zeta(p) \leq \log \chi \leq 2\eta\zeta(p-1) \ , \tag{5·4}$$

where ζ is the standard zeta function. For example, BDRG calculation of the susceptibility for $n = 11, p = 1.8, \eta = [0, 1]$ is plotted in Fig.12 with the above lower and upper boundary lines. It clearly shows that the logarithm of the susceptibility is well described by these boundary lines for weak and strong coupling regions respectively, and it moves from the lower bound to the upper bound rather quickly.

§6. Finite Range Scaling

Taking account of the inequalities presented in the previous section, now we set up the Finite Range Scaling (FRS). We take the difference of the logarithm of the susceptibility of range n system by increasing n by 1,

$$\Delta(n, p, \eta) \equiv \frac{1}{2\eta} \left[\log \chi(n) - \log \chi(n-1)\right] \ . \tag{6·1}$$

For the weak and strong boundary cases, this difference should behave as

$$\Delta^{[\mathrm{W}]} = \left(\frac{1}{n}\right)^p \ , \quad \Delta^{[\mathrm{S}]} = \left(\frac{1}{n}\right)^{p-1} \ . \tag{6·2}$$

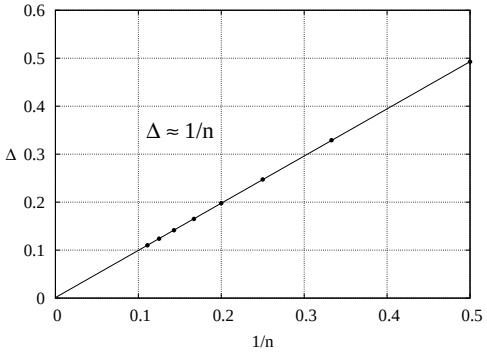

Fig. 13. Finite range scaling exponent for the strong region, $p = 2,\ \eta = 1.0$. Expected exponent is 1.0.

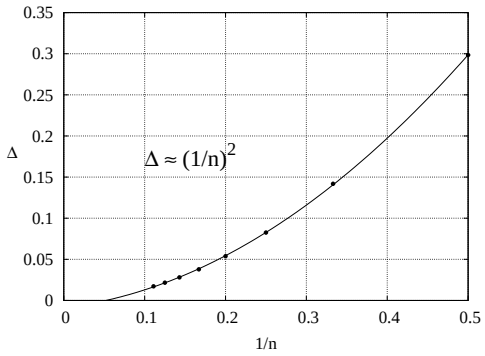

Fig. 14. Finite range scaling exponent for the weak region, $p = 2,\ \eta = 0.1$. Expected exponent is 2.0.

Referring to these boundary form, we define an FRS exponent for Δ by

$$\beta(p,\eta) \equiv \lim_{n\to\infty} \frac{\log \Delta(n,p,\eta)}{-\log n} \ . \tag{6·3}$$

We do not have a proof for the existence of this limit. It is plausible, however, to expect the existence of the asymptotic power.

We show some example of the numerical evaluation of β in case of $p = 2$. Figure 13 shows the strong coupling region of $\eta = 1.0$ and the difference Δ is well fitted by $1/n$ linear. On the other hand, Fig.14 shows a fit in the weak coupling region of $\eta = 0.1$ and the difference Δ behaves as $(1/n)^2$. Thus in this case the FRS exponent is 1.0 for the strong coupling region and 2.0 for the weak coupling region, which are perfectly consistent with the boundary values expected by the inequalities in Eq.(6·2). Furthermore for the medium coupling region, the difference Δ is well fitted by an appropriate power in $1/n$ and the power (the FRS exponent) smoothly changes for all regions of the coupling constant η. In fact, this feature holds for all p. Details of numerical results will be presented in the next section.

Then the infinite range property of the logarithm of the susceptibility (remain finite or divergent) is given by the zeta function as follows,

$$\lim_{n\to\infty} \log \chi = 2\eta \sum_{n=1}^{\infty} \left(\frac{1}{n}\right)^{\beta(p,\eta)} + [\text{finite}] = 2\eta\ \zeta[\beta(p,\eta)] + [\text{finite}] \ , \tag{6·4}$$

and therefore it is determined solely by the zeta function argument $\beta(p,\eta)$. As a real function, the zeta function $\zeta(z)$ is finite for $z > 1$ and diverges when $z \to 1_+$. Thus the condition

$$\beta(p,\eta_{\rm c}) = 1 \ , \tag{6·5}$$

determines the critical coupling constant $\eta_{\rm c}$.

On the other hand, according to the inequalities (5·4) we have the inequalities for the FRS exponent,

$$p \geq \beta(p,\eta) \geq p - 1 \ . \tag{6·6}$$

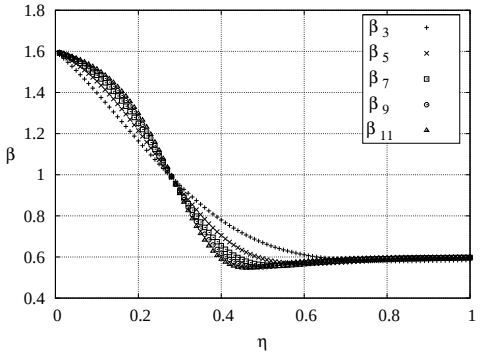

Fig. 15. Finite range scaling exponent for $p = 1.6$.

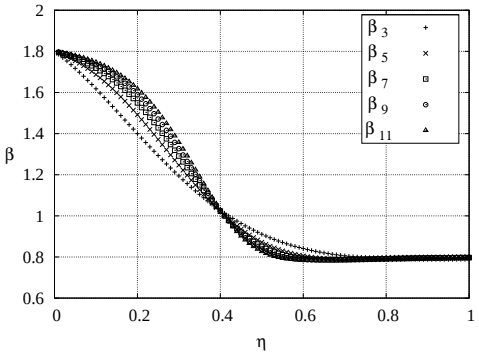

Fig. 16. Finite range scaling exponent for $p = 1.8$.

Due to the monotone property[12] of χ and therefore that of $\beta(p, \eta)$ with respect to η, $\beta(p, \eta)$ moves from p to $p - 1$ monotonically when η is changed from 0 to ∞.

Taking account of these properties about the FRS exponent, we can draw some conclusions about the phase transition property. As for $p < 1$, the susceptibility cannot be finite when $n \to \infty$ for any $\eta \neq 0$, thus the system is always ordered for any $\eta \neq 0$. To the contrary, as for $p > 2$, the susceptibility is always finite when $n \to \infty$ for any finite η, thus no ordered phase exhibits at all. As for the intermediate region of $1 < p \leq 2$, there can be a phase transition point where $\beta(p, \eta)$ crosses 1. These basic properties have already known from the very old days by other reasoning or more rigorous arguments.[7),8)] Our aim here is to evaluate the value of the critical coupling constant η_c as a function of p.

§7. Numerical Analysis

Now we numerically calculate the FRS exponent to find the critical point η_c. In actual evaluation of the exponent, we adopt the following formula,

$$\beta(n, p, \eta) \equiv -\frac{\log \Delta(n, p, \eta) - \log \Delta(n-1, p, \eta)}{\log n - \log(n-1)} \ , \tag{7·1}$$

to define $\beta(n)$.

For example, we show $\beta(n, p, \eta)$ at $p = 1.6, 1.8, 2.0$ in Figs.15, 16 and 17. As for n we take from $n = 3$ to $n = 11$. With computing resource of a desktop system, size $n = 11$ is a practical limit for overnight calculation, and in this article we work with data up to $n = 11$. First of all we confirm that the FRS exponent β changes from the weak coupling limit value p to the strong coupling limit value $p - 1$, as is predicted. The critical point η_c is located at the point $\beta = 1$. Near the critical point, β is almost independent of n. Although we do not see any reason of this stability, it is a good feature to identify the critical point. The Ohmic case $p = 2.0$ has some subtlety since its strong coupling limit value of β is 1.0 and it seems hard to evaluate the critical coupling constant with a high precision.

The FRS exponent depends on n in the region of our calculation and we expect

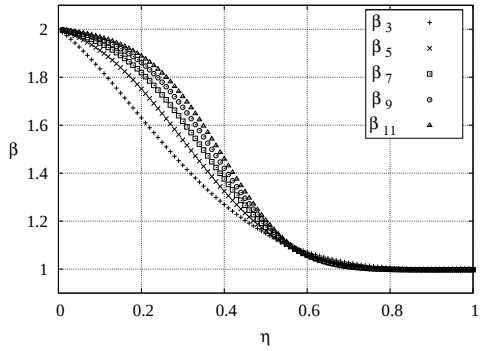

Fig. 17. Finite range scaling exponent for $p = 2.0$.

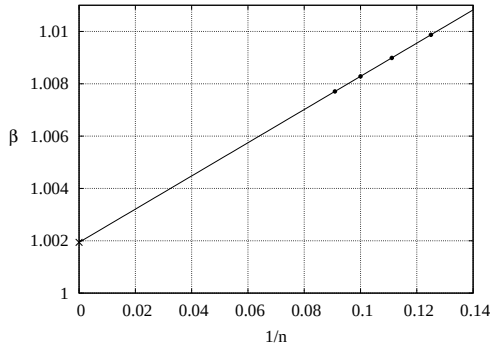

Fig. 18. $1/n$ dependence of the finite range scaling exponent, $p = 1.9, \eta = 0.5, n = 8 \sim 11$.

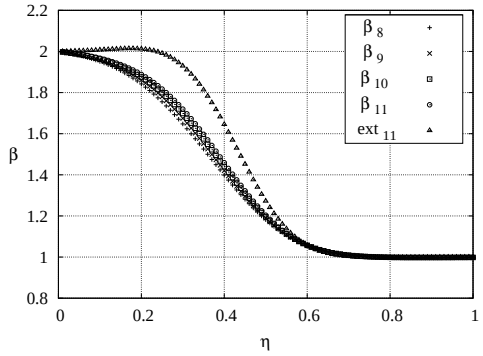

Fig. 19. Extrapolation with up to $n = 11$ data for $p = 2.0$.

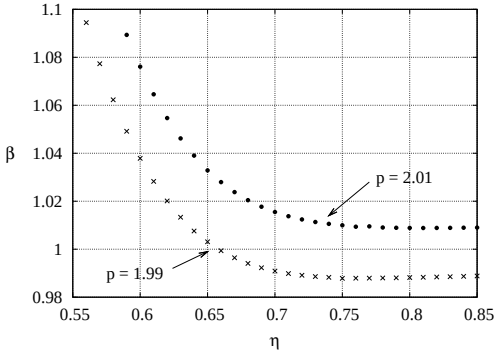

Fig. 20. Finite range scaling exponent for $p = 1.99, p = 2.01$.

that the infinite n value will be obtained by some extrapolation. To check this, in Fig.18, we plot β as a function of $1/n$ for $p = 1.9, \eta = 0.5, n = 8 \sim 11$. This plot shows that the linear extrapolation is a good choice of estimating the asymptotic value of β.

Now we show the results of the above extrapolated FRS exponent at $p = 2.0$ (the Ohmic case) in Fig.19. Extrapolation is done by using a linear function in $1/n$ with $n = 10$ and $n = 11$ data points. We notice that the phase transition becomes sharper when we adopt the extrapolated value, the right-most plot. To look at the details of the near-critical region, we plot two cases of $p = 1.99$ and $p = 2.01$ in Fig.20 where only the extrapolated values are plotted. We see that $p = 2.0$ points should exist between these two plots and the critical coupling constant would be around 0.7. We have no definite way of estimate the criticality η_c for $p = 2$ with high precision, and we just give the result for near-Ohmic case of $p = 1.99$ in the final table of results.

In Fig.21, we show an example of the detailed numerical analysis for $\beta(n, p = 1.8, \eta)$, $n = 3, 5, 7, 9, 11, \infty$ (extrapolated value using $n = 10, 11$) to estimate η_c. As is mentioned previously, according to the FRS exponent inequalities, it does change

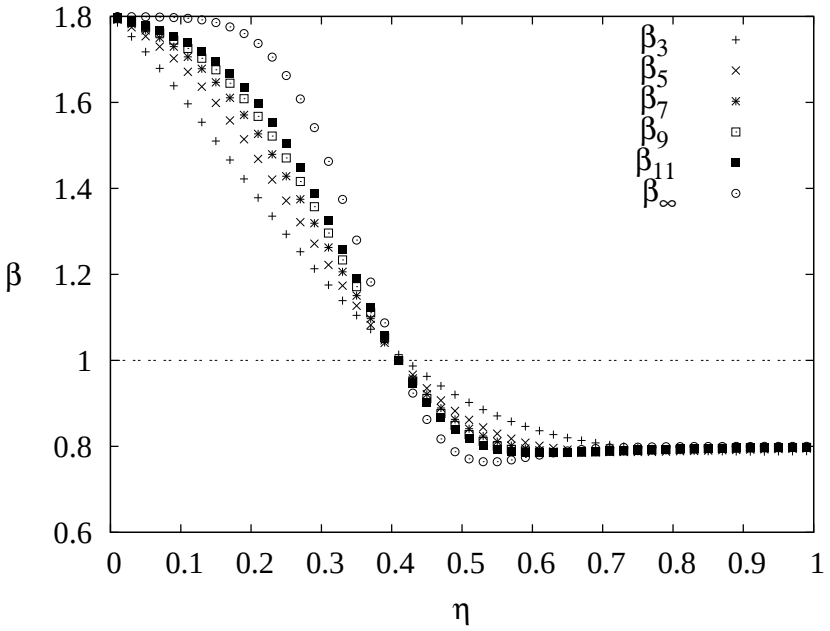

Fig. 21. FRS exponent β for $p = 1.8, \eta = [0, 1]$and $n = 3, 5, 7, 9, 11, \infty$

from the weak limit 1.8 to the strong limit 0.8 when η changes from 0 to ∞ (actually 1.0). In the midst of this monotone decrease, there is a point of $\beta = 1$ indicating the critical coupling constant η_c, which is read out to be about 0.41. Strictly speaking, the monotone property and the lower bound is broken, especially by the extrapolated values. We understand that they are fake breakings due to smallness of n.

Also we should note that around the most important region $\beta \simeq 1$, $\beta(n)$ is extremely stable against n, which is rather surprising since the critical point η_c is correctly caught even by $n = 3$ data. This stability near the criticality is common to all values of p. On the other hand, the linear extrapolation is necessary for the weak and strong regions and will make the transition shape sharper.

We have to comment on the magnetization gap which has been known to exist in this model.[9] The magnetization gap indicates that the transition is the first order and one may claim that the susceptibility does not diverge at the critical point and our method of analysis does not work. However, such claim does not matter. What we are evaluating is the susceptibility calculated on the disorder vacuum, and such quantity diverges when the spontaneous magnetization occurs. Thus we can rely on the susceptibility divergence property to discriminate the spontaneous breakdown phase boundary. Taking account of this magnetization gap feature of the transition, we guess, at the critical point, the function $\beta(\eta)$ will be singular at the criticality and jump from some value larger than 1 (the susceptibility is finite at the weak side of the criticality) to the strong limit value (there is some arguments that the susceptibility should become the upper bound value over the criticality).

Calculating the FRS exponent β for $n = 9, p = [0.9, 2.1], \eta = [0, 1]$, we have the contour plot shown in Fig.22. The thick line shows the contour of $\beta = 1$, and

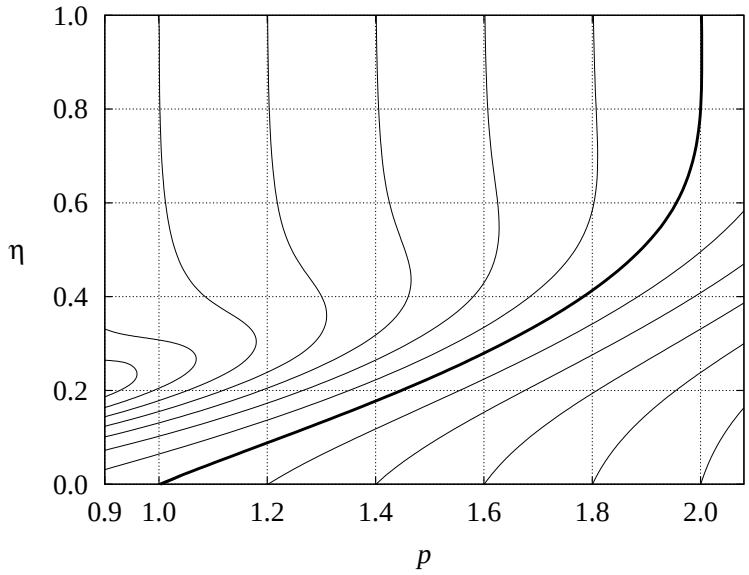

Fig. 22. Contour map of FRS exponent β for $n = 9, p = [0.9, 2.1], \eta = [0, 1]$

adjacent lines are contours with spacing 0.2. The $\beta = 1$ line is nothing but the phase boundary on the p-η plane. The lower side is the symmetric phase and the upper side is the symmetry broken phase. We see the boundary values of the β inequalities well approximate the weak and the strong region behavior for all p. We also see non-monotone structure appears more strongly for lower p, but it does not seem to affect the critical region.

Table I. The critical coupling constant $\eta_{\rm c}(p)$

p	$\eta_{\rm c}$	p	$\eta_{\rm c}$	p	$\eta_{\rm c}$	p	$\eta_{\rm c}$
1.10	0.0474(1)	1.60	0.281(1)	1.91	0.512(1)	1.96	0.582(1)
1.20	0.091(1)	1.70	0.340(1)	1.92	0.524(1)	1.97	0.602(1)
1.30	0.135(1)	1.80	0.410(1)	1.93	0.537(1)	1.98	0.626(1)
1.40	0.180(1)	1.90	0.501(1)	1.94	0.550(1)	1.99	0.657(2)
1.50	0.228(1)			1.95	0.565(1)		

The critical value $\eta_{\rm c}(p)$ is listed in Table 1. These values are evaluated by using the linearly extrapolated values of $\beta(n = \infty)$ from $n = 10, 11$. We use linear interpolation to determine the value of $\eta_{\rm c}$ from $\beta(\eta)$ plot.

For $p = 2$, it is not easy to evaluate $\eta_{\rm c}$ with high precision and here we list results for $p \leq 1.99$. Figure 23 shows our results compared with the rigorous lower bound given by Dyson and Griffiths[8),13)](DG),

$$\eta_{\rm c}(p) > 1/(2\zeta(p)) \ , \tag{7·2}$$

and with the recent high precision Monte Carlo simulation results (MC) for $p = 2$, $\eta_{\rm c} = 0.6551(6)$.[10)] Our results do not break the DG bound and actually they are very near to each other in the lower p region. The MC result and ours look consistent

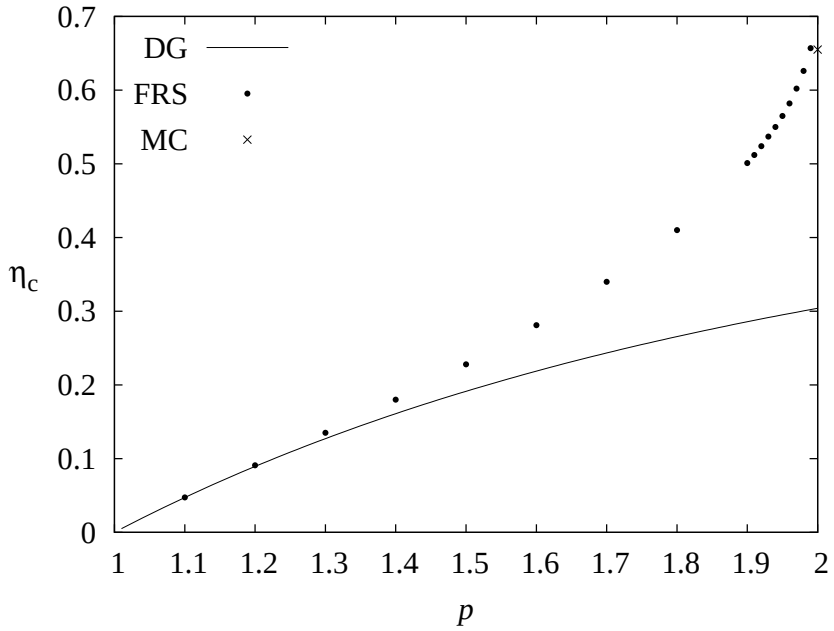

Fig. 23. Comparison of the critical coupling constant η_c as a function of p

but near $p = 2$ region should be examined in more details.

In this article we do not argue the critical exponents of the phase transition. The $\zeta(z)$ function has a simple pole at $z = 1$, and we may deduce the susceptibility critical exponent and its transition type (standard or Kosterlitz-Thouless) from detailed $\beta(p, \eta)$ behavior near η_c. It is postponed to more sophisticated analysis.

We would like to thank fruitful discussion with Atsushi Horikoshi, and valuable suggestions by Takashi Hara and Keiichi R. Ito. This research was partially supported by the Ministry of Education, Science, Sports and Culture, Grant-in-Aid for Scientific Research (B),17340070,2007.

References

1) K. G. Wilson, Rev. Mod. Phys. **47** (1975), 773.
2) A. O. Caldeira and A. J. Leggett, Phys. Rev. Lett. **46** (1981), 211; Ann. of Phys. **149** (1983), 374.
3) K. Fujikawa, S. Iso, M. Sasaki and H. Suzuki, Phys. Rev. Lett. **68** (1992), 1093; Phys. Rev. B **46** (1992), 10295.
4) K-I. Aoki, Int. J. Mod. Phys. **14** (2000), 1249;
5) K-I. Aoki, A. Horikoshi, M. Taniguchi and H. Terao, Prog. Theor. Phys. **108** (2002), 572; K-I. Aoki and A. Horikoshi, Phys. Lett. A **314** (2003), 177; Phys. Rev. A **66** (2002), 042105.
6) T. Matsuo, Y. Natsume and T. Kato, J. Phys. Soc. Jpn. **75** (2006), 103002.
7) D. Ruelle, Commun. Math. Phys. **9** (1968), 267.
8) F. J. Dyson, Commun. Math. Phys. **12** (1969), 91.
9) M. Aizenman and R. Fernández, Let. Math. Phys. **16** (1988), 39.
10) E. Luijten and H. Meßingfeld, Phys. Rev. Lett. **86** (2001), 5305.
11) K-I. Aoki, T. Kobayashi and H. Tomita in preparation.
12) R. B. Griffiths, J. Math. Phys. **8** (1967), 478.
13) R. B. Griffiths, Commun. Math. Phys. **6** (1967), 121.